Water Air Soil Pollut (2014) 225:2225
DOI 10.1007/s11270-014-2225-1

# Comparison of Response Surface Methodology and Artificial Neural Network in Optimization and Prediction of Acid Activation of Bauxsol for Phosphorus Adsorption

**Jie Ye · Panyue Zhang · Erhard Hoffmann · Guangming Zeng · Yinan Tang · Johanna Dresely · Yang Liu**

Received: 4 April 2014 / Accepted: 10 November 2014


**Abstract** Bauxsol is a chemico-physically modified product of red mud and is a promising material for the removal and recovery of phosphorus from wastewater. In this study, response surface methodology (RSM) and artificial neural network (ANN) were employed to develop prediction models and also to investigate the interactions of independent experimental factors for phosphorus adsorption onto acid-activated Bauxsol. The experimental results indicated that HCl activation was effective to improve the adsorption capacity of Bauxsol. The maximum adsorption capacity of acid-activated Bauxsol was 55.72 mg/g (as P) with HCl concentration of 10.20 mol/L, temperature of 41.00 °C, and time of 5.60 h, which increased by 10.53 and 6.62 times compared with the raw red mud and Bauxsol before acid activation, respectively. The relative importance of HCl concentration in RSM and ANN models was 51.78 and 54.25 %, respectively, which illustrated that HCl concentration played the predominant role on improving the adsorption capacity of Bauxsol. The predictive capability of RSM and ANN models was compared, and the results showed that both models provided excellent predictions with $R^2$>0.93. However, the ANN model showed the superiority over RSM for estimation capability.

J. Ye · P. Zhang (✉) · G. Zeng · Y. Liu
College of Environmental Science and Engineering,
Hunan University, Changsha 410082, China
e-mail: zhangpanyue@hnu.edu.cn

J. Ye · P. Zhang · G. Zeng · Y. Liu
Key Laboratory of Environmental Biology and Pollution Control (Hunan University), Ministry of Education,
Changsha 410082, China

J. Ye · E. Hoffmann (✉) · Y. Tang · J. Dresely
Department of Aquatic Environmental Engineering,
Karlsruhe Institute of Technology,
Karlsruhe D-76131, Germany
e-mail: Erhard.hoffmann@kit.edu

**Keywords** Response surface methodology · Artificial neural network · Prediction models · Bauxsol · Phosphorus removal

## 1 Introduction

Phosphorus is a macronutrient in the ecosystem, which is the main nutrient limiting the growth of plants and other organisms (Dong et al. 2012). However, excess discharge of phosphorus to water bodies leads to eutrophication and speeds up excess development of algae (Wang et al. 2006). Meanwhile, phosphorus is a non-renewable resource and may be depleted in 60–130 years (Steen 1998). As a consequence, the removal and recovery of phosphorus from wastewater become attractive. At present, many conventional and novel methods, including adsorption, precipitation, ion exchange, reverse osmosis, and electrodialysis, have been widely employed to remove and recover phosphorus from wastewater (Weng et al. 2011; Zhang et al. 2010; Oguz 2004). However, many of these methods are inefficient or expensive (Huang et al. 2008). Therefore, alternative

Published online: 23 November 2014

cost-effective and environmentally friendly techniques need to be developed.

Red mud, a solid waste from alumina production in Bayer process, is highly alkaline (pH 10–13) owing to its large content of sodium hydroxide (Wang et al. 2005). The amount of red mud ranges from 0.3 to more than 2 tons/ton of alumina production (Brunori et al. 2005). A large amount of red mud is generated in China each year. For example, with an $Al_2O_3$ productivity of $3.77\times10^7$ t in 2012, by-products of $1.13\times10^7$ t–$7.54\times10^7$ t was produced and discharged as slurry retaining variable water contents (National Bureau of Statistics of China 2014). Various attempts have been tried for red mud utilization (Zhang et al. 2008; Jústiz-Smith et al. 2006; Liu et al. 2009; Wang et al. 2008).

Bauxsol, a chemico-physically modified product of red mud, can be prepared by treating the caustic (pH >13) red mud with seawater, other magnesium- and calcium-rich brines, a mixture of magnesium chloride and calcium chloride, or some combination of alternatives until the pH reaches 8.2–8.6 (Genç-Fuhrman et al. 2004a; McConchie et al. 2000, 2002). Bauxsol has many advantages such as high surface area (higher than 100 $m^2$/g), moderate acid-neutralizing capacity (from 4 to 7 mol $H^+$/kg at pH 7 to approximately 14 mol $H^+$/kg at pH 5) and high metal-binding capacity (>1500 meq/kg) (Despland et al. 2010). Previous studies showed that Bauxsol could be used for treating phosphate-contaminated water based on a ligand-exchange mechanism (Akhurst et al. 2006). Therefore, Bauxsol is a potential cost-effective adsorbent for phosphorus, and further modification is necessary to achieve better effectiveness.

Response surface methodology (RSM) and artificial neural network (ANN) have been widely applied in optimizing various processes in environmental studies (Sivapathasekaran et al. 2010; Elmolla et al. 2010; Turan et al. 2013; Zinatizadeh et al. 2006; Abdessalem et al. 2008). RSM is a statistical method to build models and to analyze the interactions of independent factors. The main advantage of RSM is to reduce the number of experimental trials (Velmurugan and Muthukumar 2012). ANN simulates human intuition in making decisions and drawing conclusions when presented with information. No particular experimental design is necessary for building ANN model. In addition, ANN model is so flexible that new experimental data can be added to build a trustable ANN model (Geyikçi et al. 2012; Aghav et al. 2011). Therefore, process optimization with RSM and ANN can faster and more effectively gather experimental results than the conventional one-factor-at-a-time approach (Alim et al. 2008).

Although RSM and ANN are powerful data modeling tools, few studies have been reported to apply them in Bauxsol activation. The aim of this paper was to improve the phosphorus adsorption capacity of Bauxsol with the acid activation method. Specifically, the present work investigated the interactions of HCl concentration, temperature, and time on the acid activation of Bauxsol for phosphorus adsorption using RSM and ANN models and compared the predictive capabilities of RSM and ANN models.

## 2 Materials and Methods

### 2.1 Bauxsol Preparation

The raw red mud was obtained from Shandong Aluminum Industry Corporation in Zibo, Shandong Province of China, which was the residue of alumina production with Bayer process. Before experiments, the red mud was first sieved and the particles smaller than 100 mesh were used for further experiments.

Bauxsol was prepared by mixing the raw red mud with a solution containing calcium ion and magnesium ion, and the mixture was stirred for about 1 h until the equilibrium pH reached between 8.2 and 8.6. Then the Bauxsol slurry was dried at 50 °C overnight, ground in a mortar, and sieved through a 100-mesh sieve. Both the concentrations of calcium ion and magnesium ion were 2 mol/L.

The chemical composition of raw red mud and Bauxsol before and after acid activation is listed in Table 1. Fe and Al oxides were the main components in raw red mud and Bauxsol.

### 2.2 Activation Method

The Bauxsol powders were activated with HCl solution (5, 8, and 11 mol/L) for different times (3, 4.5, and 6 h) at various temperatures (30, 45, and 60 °C). Then the acid-activated Bauxsol slurry was centrifuged at 3000 r/min for 1 min, and the solid was separated and washed with deioned water to remove residual acid. After that, the residue was dried at 50 °C overnight. Finally, the residue was ground in a mortar and sieved through a 100-mesh sieve.

**Table 1** Chemical composition of raw red mud and Bauxsol before and after acid activation

| Constituent | Raw red mud (wt.%) | Bauxsol before acid activation (wt.%) | Bauxsol after acid activation[a] (wt.%) |
|---|---|---|---|
| $Fe_2O_3$ | 47.39 | 47.13 | 33.88 |
| $Al_2O_3$ | 22.38 | 23.62 | 30.96 |
| $Na_2O$ | 12.76 | 8.35 | 3.83 |
| $SiO_2$ | 8.88 | 9.12 | 15.52 |
| $TiO_2$ | 7.33 | 7.51 | 14.69 |
| CaO | 0.86 | 2.38 | 0.54 |
| $Cr_2O_3$ | 0.18 | 0.18 | 0.23 |
| MnO | 0.13 | 0.14 | 0.06 |
| $K_2O$ | 0.05 | 0.05 | 0.10 |
| CuO | 0.02 | 0.03 | 0.01 |
| NiO | 0.01 | 0.01 | 0.02 |
| MgO | 0.00 | 1.49 | 0.17 |

[a]The Bauxsol was activated with HCl concentration of 10.00 mol/L, temperature of 40.00 °C, and time of 5.00 h

### 2.3 Adsorption Experiments

Adsorption studies were carried out by in beaker flasks. The concentration of phosphate was 200 mg/L, and the dose of acid-activated Bauxsol was 0.5 g/L. The beaker flasks were shaken at 100 r/min for 2 h. The equilibrium time of 2 h was determined by the preliminary experiments. After equilibrium, the sample was centrifuged at 3000 r/min for 1 min and the supernatant was taken to analyze the phosphate concentration.

The amount of phosphorus adsorbed per unit of adsorbent was calculated by Eq. (1):

$$Q = \frac{\left(C_i - C_f\right)\cdot V \cdot 31}{m \cdot 95} \tag{1}$$

where $Q$ is the phosphorus adsorption capacity of Bauxsol (mg/g, as P), $C_i$ and $C_f$ is the initial and final phosphate concentration in solution (mg/L), respectively, $V$ is the solution volume (L), and $m$ is the mass of sorbent (g).

Phosphate solution was prepared by potassium dihydrogen phosphate. Magnesium ion solution and calcium ion solution were prepared by magnesium chloride hexahydrate and calcium chloride dihydrate, respectively. All chemicals were of analytical grade (Merck Co., Germany).

The adsorption temperature was controlled by a gyratory water bath shaker (model G76, New Brunswick Scientific Co. Inc., New Brunswick, USA). The equilibrium pH of the phosphorus adsorption before and after acid activation was measured with a multimeter (model MultiLine P4, WTW, Germany). The chemical composition was determined by X-ray fluorescence spectrometer (S4 Explorer, Bruker, Germany). The specific surface areas of samples were obtained by nitrogen gas sorption method (ASAP 2020V3.04H, Micromeritics, USA). Samples were equilibrated with liquid nitrogen for 10 s, followed by a degas evacuation time of 10 min. Then samples were degassed at 200 °C for 8 h at pressures between 0.005 and 0.2 atm ($P/P_o$). Phosphate concentration was determined via the spectrophotometric method DIN-EN-ISO-15681-1 with the QuikChem 8500 flow injection analysis system (Lachat Instruments Inc., USA). All experiments were conducted in triplicate, and the average values were used for data analysis.

### 2.4 Experimental Design and Data Analysis for Acid Activation of Bauxsol

#### *2.4.1 RSM Modeling*

The design and analysis of variables were evaluated using Design-Expert V8.0 and MatLab 10.0. According to the results from preliminary experiments with one-factor-at-a-time method, three main factors for Bauxsol activation were chosen: HCl concentration, temperature, and time.

Box-Behnken design (BBD) was used to accurately describe linear, quadratic, and interaction in the RSM model. In comparison with the central composite design and the full-factorial design, BBD is more labor efficient and does not contain combinations for which all factors are simultaneously at their highest or lowest levels. So, the BBD is useful in avoiding experiments performed under extreme conditions (Ferreira et al. 2007). Therefore, RSM with BBD was applied to optimize the three factors in this study. The preliminary experiments with one-factor-at-a-time method were done to determine a narrower range of the three factors, and the experimental design levels of chosen factors are given in Table 2.

The quadratic equation model for predicting the optimal operating factors can be expressed as Eq. (2):

$$Y = \beta_0 + \sum_{i=1}^{k} \beta_i X_i + \sum_{i=1}^{k} \beta_{ii} X_i^2 + \sum_{i_{i \le j}}^{k} \sum_{j}^{k} \beta_{ij} X_i X_j + \cdots + e \tag{2}$$

where $Y$ is the predicted response, $X_i, X_j, \ldots, X_k$ are the input variables, $X_i^2, X_j^2, \ldots, X_k^2$ are the square effects, $X_iX_j$, $X_iX_k$ and $X_jX_k$ are the interaction effects, $\beta_0$ is the intercept, $\beta_i (i=1,2,\ldots,k)$ is the linear effect, $\beta_{ii} (i=1,2,\ldots,k)$ is the squared effect, $\beta_{ij} (i=1,2,\ldots,k; j=1,2,\ldots,k)$ is the interaction effect, and $e$ is a random error (Turan et al. 2013).

*2.4.2 ANN Modeling*

Feed forward ANN was chosen because it is suitable for modeling the relationship between input data and output variable (Witek-Krowiak et al. 2014). The number of hidden neurons in ANN modeling is important. Too many neurons can extend the time necessary for training the network, while too few neurons may not be sufficient to train the network at all (Guo et al. 2014). In this paper, the performance of ANN with varying number of neurons (1–12) in the hidden layer was investigated and the results demonstrated that five hidden neurons were the best.

The selection of an appropriate learning method is also an essential part for modeling with ANN, because successful network training is associated with a continuous improvement of the network by minimizing the error function, which is performed by training algorithm (Witek-Krowiak et al. 2014). The most widely used neural network is back-propagation (BP), a descent algorithm, which attempts to minimize the error at each iteration (Turan et al. 2011).

Therefore, a three-layered feed-forward ANN trained by the back-propagation algorithm was proposed in this study (Fig. 1). The training parameters used in this model are listed in Table 3.

In a dependent-independent variable modeling approach, it is necessary to assess the relative importance of each independent variable in a model (Desai et al. 2008). In this study, the values of Pareto analysis ($P$) and importance ($I$) were chosen to value the importance of each independent factor in RSM and ANN models, respectively. They were calculated by Eqs. (3) and (4) (Haaland 1989; Singh et al. 2009):

$$P_i = \left( \frac{\beta_i^2}{\sum_{i=1}^{k} \beta_i^2} \right) \tag{3}$$

$$I_i = \frac{\sum_{j=1}^{n_h} \mathrm{ABS}\left(w_{ji}\right)}{\sum_{k=1}^{n_v} \left( \sum_{j=1}^{n_h} \mathrm{ABS}\left(w_{ji}\right)_k \right)} \tag{4}$$

where $n_h$ is the number of hidden nodes, $n_v$ is the number of input variables, $w_{ji}$ is the connection weight from the $i$th input node to $j$th hidden node, and ABS demotes the absolute value of the function.

The performance of RSM and ANN models was determined based on the values of the root mean squared error (RMSE), mean absolute percentage error (MAPE), and coefficient of determination ($R^2$). They were calculated by Eqs. (5), (6), and (7) (Desai et al. 2008):

$$\mathrm{RMSE} = \left( \frac{1}{n} \sum_{i=1}^{n} \left( y_i - y_{di} \right)^2 \right)^{1/2} \tag{5}$$

**Table 2** Experimental levels of independent variables

| Variables | Levels | | |
|---|---|---|---|
| | Low level (−1) | Medium level (0) | High level (+1) |
| HCl concentration (mol/L) | 5.00 | 8.00 | 11.00 |
| Temperature (°C) | 30.00 | 45.00 | 60.00 |
| Time (h) | 3.00 | 4.50 | 6.00 |

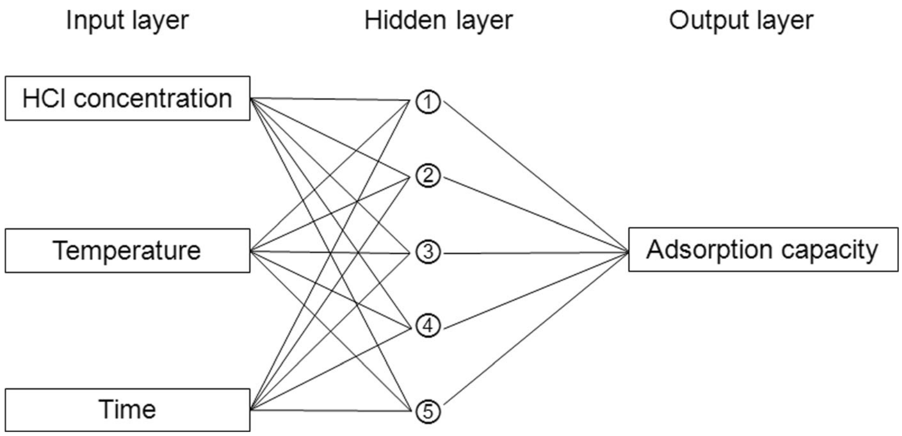


**Fig. 1** Schematic representation of a (3–5–1) neural network (with three neurons in the input layer, five in the hidden layer, and one in the output layer)

$$\mathrm{MAPE} = \frac{1}{n}\sum_{i=1}^{n} \left| \left(\frac{y_i - y_{di}}{y_{di}}\right) \right| \times 100 \qquad (6)$$

$$R^2 = \frac{\left(\sum_{i=1}^{n} (y_{di} - y_{di}') (y_i - y_i')\right)^2}{\left(\sum_{i=1}^{n} (y_{di} - y_{di}')^2 (y_i - y_i')\right)^2} \qquad (7)$$

where the symbol ' represents the average of related values, $n$ is the number of points, $y_i$ is the predicted value and $y_{di}$ is the measured value.

## 3 Results and Discussion

### 3.1 Modeling with RSM

A BBD with a total of 17 experiments was employed for RSM. Table 4 reports the experimental and predicted values of the adsorption capacity of acid-activated Bauxsol.

According to the results, the coefficients of polynomial model were attained and expressed by Eq. (8):

$$Y = 50.25 + 16.12X_1 - 3.90X_2 + 1.46X_3 - 2.65X_1X_2 - 2.12X_1X_3 - 1.91X_2X_3 - 13.32{X_1}^2 - 5.52{X_2}^2 - 1.22{X_3}^2 \qquad (8)$$

in which $X_1$ is the HCl concentration, $X_2$ is the temperature, $X_3$ is the time, and $Y$ is the phosphorus adsorption capacity.

Coefficient of determination ($R^2$) presents the quality of polynomial model (Zarei et al. 2010). The predicted $R^2$ considers all effects, and adjusted $R^2$ considers only square effects and interaction effects between two input variables. The predicted $R^2$ and adjusted $R^2$ in this study was 0.9455 and 0.9867, respectively, indicating that only 5.45 % of total variations could not be explained by the model. “Adeq Precision” measures the ratio of signal to noise, and a ratio greater than 4 is desirable. The ratio was 31.84 in this study, indicating an adequate signal. Therefore, RSM model could be used to navigate the design space (Kuehl 2000).

**Table 3** ANN training parameters

| Parameter | Value |
|---|---|
| Number of input nodes | 3 |
| Number of output nodes | 1 |
| Number of hidden neurons | 5 |
| Maximum number of epochs | 300 |
| Learning rate | 0.01 |
| Learning rule | Back-propagation |
| Error goal | 0.0001 |

Analysis of variance (ANOVA) for the response surface quadratic model is shown in Table 5. The model $F$ value of 132.59 implied that the RSM model was significant. The $p$ values are used to check the significance of each of the coefficients. The $p$ values less than 0.05 indicate that the RSM model terms are significant. In this study, $X_1$, $X_2$, $X_3$, $X_1X_2$, $X_1X_3$, ${X_1}^2$, and ${X_2}^2$ were

**Table 4** BBD matrix and neural network training set

| Run | $X_1$ (mol/L) | | $X_2$ (°C) | | $X_3$ (h) | | $Y$ (mg/g) | |
|---|---|---|---|---|---|---|---|---|
| | Uncoded | Coded | Uncoded | Coded | Uncoded | Coded | Measured | Predicted |
| 1 | 5.00 | −1 | 45.00 | 0 | 6.00 | 1 | 22.23±0.34 | 23.01 |
| 2 | 8.00 | 0 | 45.00 | 0 | 4.50 | 0 | 50.07±0.11 | 50.19 |
| 3 | 8.00 | 0 | 45.00 | 0 | 4.50 | 0 | 48.27±0.25 | 50.19 |
| 4 | 5.00 | −1 | 60.00 | 1 | 4.50 | 0 | 13.67±0.30 | 14.15 |
| 5 | 11.00 | 1 | 45.00 | 0 | 3.00 | −1 | 53.43±0.08 | 52.44 |
| 6 | 11.00 | 1 | 60.00 | 1 | 4.50 | 0 | 40.90±0.40 | 41.18 |
| 7 | 8.00 | 0 | 60.00 | 1 | 6.00 | 1 | 40.46±0.09 | 39.18 |
| 8 | 8.00 | 0 | 45.00 | 0 | 4.50 | 0 | 51.90±0.26 | 50.19 |
| 9 | 8.00 | 0 | 60.00 | 1 | 3.00 | −1 | 39.19±0.27 | 39.93 |
| 10 | 11.00 | 1 | 45.00 | 0 | 6.00 | 1 | 49.91±0.57 | 51.45 |
| 11 | 8.00 | 0 | 45.00 | 0 | 4.50 | 0 | 51.47±0.82 | 50.19 |
| 12 | 8.00 | 0 | 30.00 | −1 | 3.00 | −1 | 42.72±0.39 | 43.83 |
| 13 | 11.00 | 1 | 30.00 | −1 | 4.50 | 0 | 54.47±0.27 | 54.29 |
| 14 | 5.00 | −1 | 45.00 | 0 | 3.00 | −1 | 17.26±0.83 | 15.95 |
| 15 | 5.00 | −1 | 30.00 | −1 | 4.50 | 0 | 16.62±0.31 | 16.38 |
| 16 | 8.00 | 0 | 30.00 | −1 | 6.00 | 1 | 51.64±0.36 | 50.64 |
| 17 | 8.00 | 0 | 45.00 | 0 | 4.50 | 0 | 49.53±0.49 | 50.19 |

significant model terms. $X_1$ and $X_1^2$ ($p<0.0001$) were the most significant terms for the phosphorus adsorption capacity.

In regard to the relative importance of each input variable, the values of $P$ showed that HCl concentration ($X_1$) (51.78 %) and $X_1^2$ (35.36 %) had the greatest effects on the phosphorus adsorption capacity.

Contour plots were obtained based on the effects of two factors. Specifically, these plots showed how HCl concentration, temperature, and time related to the phosphorus adsorption capacity of acid-activated Bauxsol. Figure 2 shows the contour plots for the phosphorus adsorption capacity of acid-activated Bauxsol as a function of HCl concentration and temperature for an

**Table 5** Analysis of variance (ANOVA) for the RSM model

| Factor | Sum of squares | $df$ | Mean square | $F$ value | $p$ value prob>$F$ | Remark |
|---|---|---|---|---|---|---|
| Model | 3209.24 | 9 | 356.58 | 132.59 | <0.0001 | Significant |
| $X_1$ | 2077.65 | 1 | 2077.65 | 772.56 | <0.0001 | |
| $X_2$ | 121.99 | 1 | 121.99 | 45.36 | 0.0003 | |
| $X_3$ | 16.94 | 1 | 16.94 | 6.30 | 0.0404 | |
| $X_1X_2$ | 28.20 | 1 | 28.20 | 10.48 | 0.0143 | |
| $X_1X_3$ | 18.01 | 1 | 18.01 | 6.70 | 0.0361 | |
| $X_2X_3$ | 14.63 | 1 | 14.63 | 5.44 | 0.0524 | |
| $X_1^2$ | 746.66 | 1 | 746.66 | 277.64 | < 0.0001 | |
| $X_2^2$ | 128.23 | 1 | 128.23 | 47.68 | 0.0002 | |
| $X_3^2$ | 6.31 | 1 | 6.31 | 2.35 | 0.1694 | |
| Residual | 18.83 | 7 | 2.69 | | | |
| Cor. total | 3228.07 | 16 | | | | |

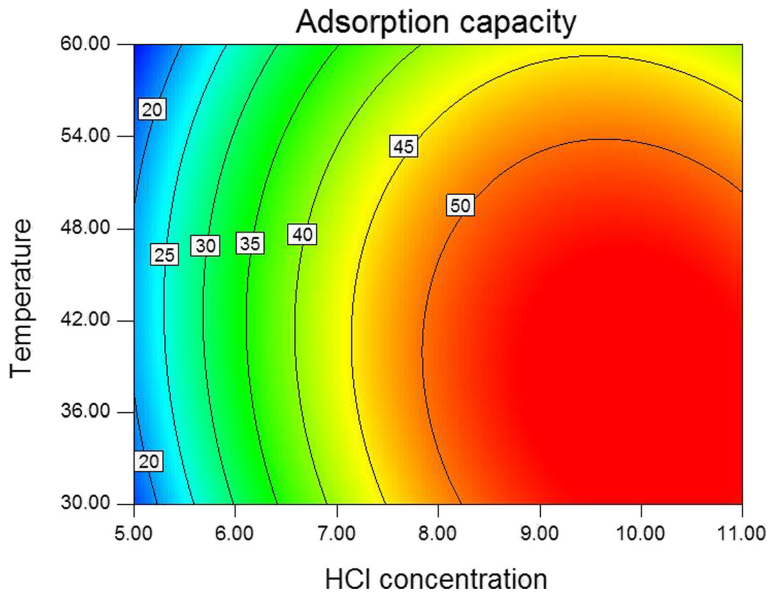


**Fig. 2** Contour plots of response surface for effect of HCl concentration and temperature on phosphorus adsorption capacity of acid-activated Bauxsol (time=4.50 h)

activation time of 4.50 h. Clearly, the adsorption capacity of acid-activated Bauxsol reached the highest when HCl concentration was about 10.00 mol/L under all conditions. On the other hand, temperature showed no significant effect on the adsorption capacity.

Appropriate HCl concentration can enhance the positive charge on metal oxide surface of Bauxsol, as shown in Eqs. (9), (10), (11), (12), (13), (14), (15), and (16):

$$Al_2O_3 + 6HCl = 2AlCl_3 + 3H_2O \quad \text{(dissolution)} \tag{9}$$

$$Fe_2O_3 + 6HCl = 2FeCl_3 + 3H_2O \quad \text{(dissolution)} \tag{10}$$

$$AlCl_3 + H_2O \leftrightarrow {}^{+}Al(OH)^{+} + H^{+} + 3Cl^{-} \quad \text{(hydrolysis)} \tag{11}$$

$$FeCl_3 + H_2O \leftrightarrow {}^{+}F\ + e(OH)^{+} + H^{+} + 3Cl^{-} \quad \text{(hydrolysis)} \tag{12}$$

$$R^{-} + {}^{+}Al(OH)^{+} \leftrightarrow R\text{-}Al(OH)^{+} \quad \text{(polymerization)} \tag{13}$$

$$R^{-} + {}^{+}Fe(OH)^{+} \leftrightarrow R-Fe(OH)^{+} \quad \text{(polymerization)} \tag{14}$$

$$nR-Al(OH)^{+} + L^{n-} \leftrightarrow nR-AlL^{+} + nOH^{-} \quad \text{(adsorption)} \tag{15}$$

$$nR-Fe(OH)^{+} + L^{n-} \leftrightarrow nR-FeL^{+} + nOH^{-} \quad \text{(adsorption)} \tag{16}$$

where $R$ is a surface, $L^{n-}$ is a ligand (e.g., $PO_4^{3-}$, $HPO_4^{2-}$, $H_2PO_4^{-}$), and $R-Al(OH)^{+}$ and $R-Fe(OH)^{+}$ are surface species (Genç-Fuhrman et al. 2004b; Zhao et al. 2011).

With the increase of HCl concentration, the amount of $H^{+}$ increased, which stimulated the formation of Al(III) and Fe(III) ions through Eqs. (9) and (10). The more metal ions were extracted from Bauxsol, the more hydrolysis reactions of Al(III) and Fe(III) ions would occur, as shown in Eqs. (11) and (12). The higher the polymerization extent by hydrolyzing Al(III) and Fe(III) was, the stronger charge-neutralizing and adsorption-bridging capacity acid-activated Bauxsol presented; so the acid-activated Bauxsol had better phosphorus adsorption capacity (Eqs. 13 and 14). The ligand-exchange reactions occurred with the release of $OH^{-}$ ions (Eqs. 15 and 16), so the equilibrium pH after phosphorus adsorption increased to 3.65 and 4.71 for Bauxsol before and after acid activation, respectively, when the initial pH was 3.32. Moreover, the acid-activated Bauxsol displayed a larger BET surface area of 80.63 $m^2/g$ than raw red mud (35.46 $m^2/g$) and Bauxsol before acid activation (40.67 $m^2/g$), which is similar to that of

Genç-Fuhrman et al. (2004b). The increased surface area and consequent adsorption capacity might be attributed to the generation of amorphous and semi-amorphous materials of Fe and Al after the acid activation (Freire et al. 2012), because Fe and Al were the main components of the raw red mud, and the Al content increased substantially after acid activation. However, if the HCl concentration was too high (more than about 10.00 mol/L), the reactions shown in Eqs. (11) and (12) would be impelled to conduct reversely. As a result, the formation of $^{+}Al(OH)^{+}$ and $^{+}Fe(OH)^{+}$ would decrease and the phosphorus adsorption capacity of Bauxsol would decrease consequently.

Figure 3 illustrates the effect of HCl concentration and time upon the phosphorus adsorption capacity of acid-activated Bauxsol for an activation temperature of 45.00 °C. Similarly, the phosphorus adsorption capacity of acid-activated Bauxsol increased with HCl concentration increasing but was not impacted by the activation time.

The phosphorus adsorption capacity of acid-activated Bauxsol for HCl concentration of 8.00 mol/L as a function of temperature and time is depicted in Fig. 4. At first, the phosphorus adsorption capacity of acid-activated Bauxsol increased with the temperature and time increasing and then decreased. Specifically, longer reaction time could enhance the reaction extent between Bauxsol and HCl (Zhao et al. 2011), but it would also decrease the stability of Bauxsol (Liu et al. 2007). Meanwhile, temperature influenced the particle transport processes or particle collision rates because of the viscosity change, and thus influenced the mixing energy dissipated in water. With the temperature increasing, the viscosity decreased, leading to rapid-mixing conditions. Better mixing led to homogeneous distribution of metal species, which accelerated the dissolution, hydrolysis, polymerization, and adsorption reactions. As a result, better phosphorus adsorption capacity was achieved (Zhang and Pan 2005; Wei et al. 2009). However, the stability of Bauxsol could also decrease with increasing temperature.

A multiple response method in Design-Expert V8.0 was applied for the optimization of any combination of HCl concentration, temperature, time, and phosphorus adsorption capacity. The results showed that maximum adsorption capacity of acid-activated Bauxsol was 55.72 mg/g with an HCl concentration of 10.20 mol/L, temperature of 41.00 °C, and time of 5.60 h, which increased by 10.53 and 6.62 times compared with the raw red mud and Bauxsol before acid activation (4.83 and 7.31 mg/g), respectively.

### 3.2 Modeling with ANN

The selected ANN provided a best-fit model for the training data (Table 3). The value of $R^2$ was 0.997, and the value of RMSE was 0.715.

The values of *I* were chosen to value the importance of each independent variable in ANN model. The results showed that in the ANN model, all the input variables

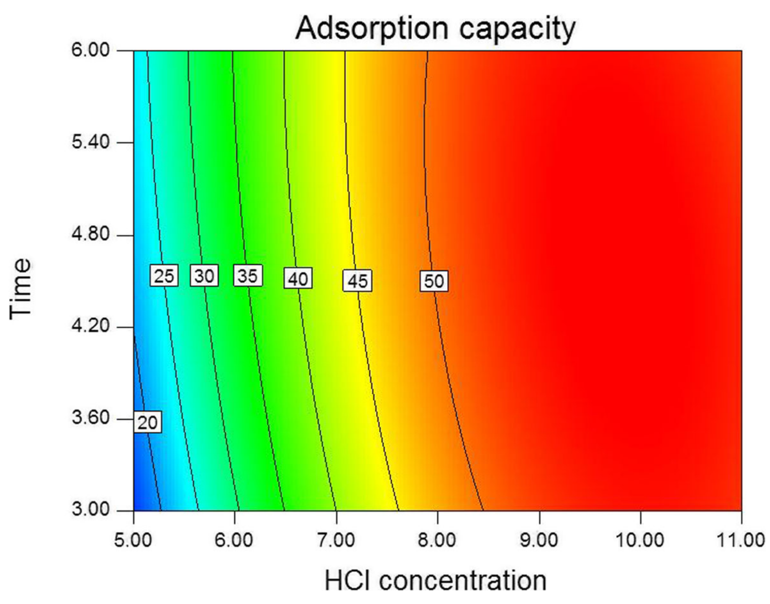


**Fig. 3** Contour plots of response surface for effect of HCl concentration and time on phosphorus adsorption capacity of acid-activated Bauxsol (temperature=45.00 °C)

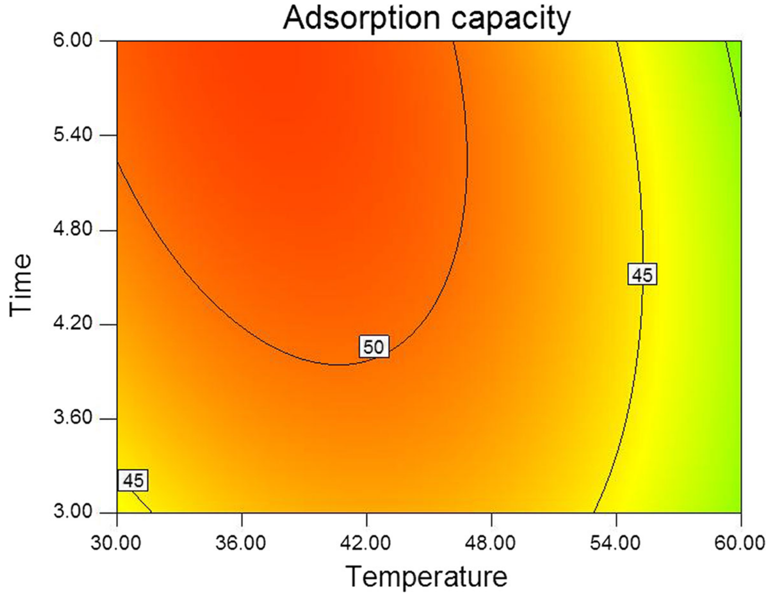


**Fig. 4** Contour plots of response surface for effect of temperature and time on phosphorus adsorption capacity of acid-activated Bauxsol (HCl concentration=8.00 mol/L)

participated significantly (>10 %). Specifically, HCl concentration was the most effective factor among all variables (54.25 %). The importance of activation temperature was higher than that of activation time, which was consistent with the results from the RSM model.

### 3.3 Performance of RSM and ANN Models

In order to test the validity of results from RSM and ANN models, experimental parameters according to the design matrix given in Table 6 were used. Predicted adsorption capacities and residuals for both approaches were also shown in Table 6.

Comparison of RSM and ANN models statically, it was evident that the RSM and ANN models provided good quality predictions in this study. The $R^2$ of RSM and ANN for the data in Table 5 were 0.939 and 0.999, respectively. The RMSE by RSM and ANN were 3.647 and 0.390, and the values of MAPE were 6.895 and 1.037, respectively. However, these results also showed that the ANN model had the superiority over RSM model for estimation of phosphorus adsorption capability of acid-activated Bauxsol.

## 4 Conclusion

In this study, the interactions of HCl concentration, temperature, and time on the acid activation of Bauxsol for phosphorus adsorption were investigated using RSM and ANN. The results indicated that acid activation was useful for improving the phosphorus adsorption capacity of Bauxsol and the maximum adsorption capacity of acid-activated Bauxsol was 55.72 mg/g (as P) with HCl concentration of 10.20 mol/L, temperature of 41.00 °C, and time of 5.60 h. The relative importance of HCl

**Table 6** Validation set

| Run | $X_1$ (mol/L) | $X_2$ (°C) | $X_3$ (h) | Adsorption capacity (mg/g) | RSM | | ANN | |
|---|---|---|---|---|---|---|---|---|
| | | | | | Predicted (mg/g) | Residual (mg/g) | Predicted (mg/g) | Residual (mg/g) |
| 1 | 5.00 | 30.00 | 6.00 | 19.75±0.25 | 20.81 | −1.06 | 20.11 | −0.36 |
| 2 | 5.00 | 60.00 | 6.00 | 15.85±0.15 | 14.49 | 1.36 | 15.63 | 0.22 |
| 3 | 8.00 | 30.00 | 3.00 | 41.96±0.61 | 44.04 | −2.08 | 42.72 | −0.76 |
| 4 | 8.00 | 60.00 | 4.50 | 47.93±0.39 | 40.82 | 7.11 | 47.95 | −0.02 |
| 5 | 11.00 | 45.00 | 4.50 | 50.11±1.28 | 53.05 | −2.94 | 50.17 | −0.06 |

concentration to RSM and ANN models were 51.78 and 54.25 %, respectively, which illustrated that HCl concentration had the greatest effect on the acid activation of Bauxsol for phosphorus adsorption. RSM and ANN methodologies were compared for their predictive capabilities, and the results showed that both of them provided good-quality predictions with $R^2>0.93$. However, the ANN showed better prediction accuracy than RSM.

**Acknowledgments** The authors are thankful to the China Scholarship Council (CSC), the National Natural Science Foundation of China (51178047, 51378190, 51039001), and Furong Scholar of Hunan Province for supporting.

## References

Abdessalem, A. K., Oturan, N., Bellakhal, N., Dachraoui, M., & Oturan, M. A. (2008). Experimental design methodology applied to electro-Fenton treatment for degradation of herbicide chlortoluron. *Applied Catalysis B Environmental, 78*(3–4), 334–341.

Aghav, R. M., Kumar, S., & Mukherjee, S. N. (2011). Artificial neural network modeling in competitive adsorption of phenol and resorcinol from water environment using some carbonaceous adsorbents. *Journal of Hazardous Materials, 188*(1–3), 67–77.

Akhurst, D. J., Jones, G. B., Clark, M., & McConchie, D. (2006). Phosphate removal from aqueous solutions using neutralised bauxite refinery residues (Bauxsol™). *Environmental Chemistry, 3*(1), 65–74.

Alim, M. A., Lee, J. H., Akoh, C. C., Choi, M. S., Jeon, M. S., Shin, J. A., & Lee, K. T. (2008). Enzymatic transesterification of fractionated rice bran oil with conjugated linoleic acid: optimization by response surface methodology. *LWT - Food Science and Technology, 41*(5), 764–770.

Brunori, C., Cremisini, C., Massanisso, P., Pinto, V., & Torricelli, L. (2005). Reuse of a treated red mud bauxite waste: studies on environmental compatibility. *Journal of Hazardous Materials, 117*(1), 55–63.

Desai, K. M., Survase, S. A., Saudagar, P. S., Lele, S. S., & Singhal, R. S. (2008). Comparison of artificial neural network (ANN) and response surface methodology (RSM) in fermentation media optimization: case study of fermentative production of scleroglucan. *Biochemical Engineering Journal, 41*(3), 266–273.

Despland, L. M., Clark, M. W., Aragno, M., & Vancov, T. (2010). Minimising alkalinity and pH spikes from Portland cement-bound Bauxsol (seawater-neutralized red mud) pellets for pH circum-neutral waters. *Environmental Science & Technology, 44*(6), 2119–2125.

Dong, H., Guan, X., & Lo, I. M. C. (2012). Fate of As(V)-treated nano zero-valent iron: determination of arsenic desorption potential under varying environmental conditions by phosphate extraction. *Water Research, 46*(13), 4071–4080.

Elmolla, E. S., Chaudhuri, M., & Eltoukhy, M. M. (2010). The use of artificial neural network (ANN) for modeling of COD removal from antibiotic aqueous solution by the Fenton process. *Journal of Hazardous Materials, 179*(1–3), 127–134.

Ferreira, S. C., Bruns, R. E., Ferreira, H. S., Matos, G. D., David, J. M., Brandao, G. C., Silva, E. G. P., Portugal, L. A., Reis, P. S., Souza, A. S., & Santos, W. N. L. (2007). Box-Behnken design: an alternative for the optimization of analytical methods. *Analytica Chimica Acta, 597*(2), 179–186.

Freire, T. S. S., Clark, M. W., Comarmond, M. J., Payne, T. E., Reichelt-Brushett, A. J., & Thorogood, G. J. (2012). Electroacoustic isoelectric point determinations of bauxite refinery residues: different neutralisation techniques and minor mineral effects. *Langmuir, 28*(32), 11802–11811.

Genç-Fuhrman, H., Tjell, J. C., & McConchie, D. (2004a). Adsorption of arsenic from water using activated neutralized red mud. *Environmental Science & Technology, 38*(8), 2428–2434.

Genç-Fuhrman, H., Tjell, J. C., & McConchie, D. (2004b). Increasing the arsenate adsorption capacity of neutralized red mud (Bauxsol). *Journal of Colloid and Interface Science, 271*(2), 313–320.

Geyikçi, F., Kılıç, E., Çoruh, S., & Elevli, S. (2012). Modelling of lead adsorption from industrial sludge leachate on red mud by using RSM and ANN. *Chemical Engineering Journal, 183*, 53–59.

Guo, Y. M., Liu, Y. G., Zeng, G. M., Hu, X. J., Xu, W. H., Liu, Y. Q., Liu, S. M., Sun, H. S., Ye, J., & Huang, H. J. (2014). An integrated treatment of domestic wastewater using sequencing batch biofilm reactor combined with vertical flow constructed wetland and its artificial neural network simulation study. *Ecological Engineering, 64*, 18–26.

Haaland, D. P. (1989). *Experimental design in biotechnology.* New York: Marcel Dekker, Inc.

Huang, W., Wang, S., Zhu, Z., Li, L., Yao, X., Rudolph, V., & Haghseresht, F. (2008). Phosphate removal from wastewater using red mud. *Journal of Hazardous Materials, 158*(1), 35–42.

Jústiz-Smith, N., Buchanan, V. E., & Oliver, G. (2006). The potential application of red mud in the production of castings. *Materials Science and Engineering A, 420*(1–2), 250–253.

Kuehl, R. O. (2000). *Design of experiments: statistical principles of research design and analysis* (2nd ed.). Pacific Grove: Duxbury press.

Liu, C., Li, Y., Luan, Z., Chen, Z., Zhang, Z., & Jia, Z. (2007). Adsorption removal of phosphate from aqueous solution by active red mud. *Journal of Environmental Sciences, 19*(10), 1166–1170.

Liu, W., Yang, J., & Xiao, B. (2009). Application of Bayer red mud for iron recovery and building material production from alumosilicate residues. *Journal of Hazardous Materials, 161*(1), 474–478.

McConchie, D., Clark, M., & Davies-McConchie, F. (2000). Processes for water treatment. International Parent PCT/AU01/01383.

McConchie, D., Clark, M., Davies-McConchie, F., & Ryffel, T. (2002). Processes for the treatment of a waste material having a high pH and/or alkalinity. International Patent PCT/AU03/00865.

National Bureau of Statistics of China. (2014). Available at: http://data.stats.gov.cn/search/keywordlist2;jsessionid=342489F18B17DF162DF276E2B5F3729A?keyword=%E6%B0%A7%E5%8C%96%E9%93%9days.

Oguz, E. (2004). Removal of phosphate from aqueous solution with blast furnace slag. *Journal of Hazardous Materials, 114*(1–3), 131–137.

Singh, K. P., Basant, A., Malik, A., & Jain, G. (2009). Artificial neural network modeling of the river water quality-a case study. *Ecological Modelling, 220*(6), 888–895.

Sivapathasekaran, C., Mukherjee, S., Ray, A., Gupta, A., & Sen, R. (2010). Artificial neural network modeling and genetic algorithm based medium optimization for the improved production of marine biosurfactant. *Bioresource Technology, 101*(8), 2884–2887.

Steen, I. (1998). Management of a non-renewable resource. *Phosphorus and Potassium, 217*, 25–31.

Turan, N. G., Mesci, B., & Ozgonenel, O. (2011). The use of artificial neural networks (ANN) for modeling of adsorption of Cu (II) from industrial leachate by pumice. *Chemical Engineering Journal, 171*(3), 1091–1097.

Turan, N. G., Mesci, B., & Ozgonenel, O. (2013). Response surface modeling of Cu(II) removal from electroplating waste by adsorption: application of Box-Behnken experimental design. *Clean Soil Air Water, 41*(3), 304–312.

Velmurugan, R., & Muthukumar, K. (2012). Ultrasound-assisted alkaline pretreatment of sugarcane bagasse for fermentable sugar production: optimization through response surface methodology. *Bioresource Technology, 112*, 293–299.

Wang, S., Boyjoo, Y., Choueib, A., & Zhu, Z. H. (2005). Removal of dyes from aqueous solution using fly ash and red mud. *Water Research, 39*(1), 129–138.

Wang, J., Song, Y., Yuan, P., Peng, J., & Fan, M. (2006). Modeling the crystallization of magnesium ammonium phosphate for phosphorus recovery. *Chemosphere, 65*(7), 1182–1187.

Wang, S., Ang, H. M., & Tadé, M. O. (2008). Novel applications of red mud as coagulant, adsorbent and catalyst for environmentally benign processes. *Chemosphere, 72*(11), 1621–1635.

Wei, L., Qiu, H., Zhang, J., Yu, Y., Yang, K., Liu, Z., & Ding, G. (2009). Characteristic of a novel composite inorganic polymer coagulant-PFAC prepared by hydrochloric pickle liquor. *Journal of Hazardous Materials, 162*(1), 174–179.

Weng, L., Vega, F. A., & Riemsdijk, W. H. V. (2011). Competitive and synergistic effects in pH dependent phosphate adsorption in soils: LCD modeling. *Environmental Science & Technology, 45*(19), 8420–8428.

Witek-Krowiak, A., Chojnacka, K., Podstawczyk, D., Dawiec, A., & Pokomeda, K. (2014). Application of response surface methodology and artificial neural network methods in modelling and optimization of biosorption process. *Bioresource Technology*. doi:10.1016/j.biortech.2014.01.021.

Zarei, M., Niaei, A., Salari, D., & Khataee, A. (2010). Application of response surface methodology for optimization of peroxi-coagulation of textile dye solution using carbon nanotube–PTFE cathode. *Journal of Hazardous Materials, 173*(1–3), 544–551.

Zhang, Y. N., & Pan, Z. H. (2005). Characterization of red mud thermally treated at different temperatures. *Journal of Jinan University (Science and Technology), 19*, 35–38.

Zhang, S., Liu, C., Luan, Z., Peng, X., Ren, H., & Wang, J. (2008). Arsenate removal from aqueous solutions using modified red mud. *Journal of Hazardous Materials, 152*(2), 486–492.

Zhang, T., Ding, L., Ren, H., Guo, Z., & Tan, J. (2010). Thermodynamic modeling of ferric phosphate precipitation for phosphorus removal and recovery from wastewater. *Journal of Hazardous Materials, 176*(1–3), 444–450.

Zhao, Y., Zhang, L., Ni, F., Xi, B., Xia, X., Peng, X., & Luan, Z. (2011). Evaluation of a novel composite inorganic coagulant prepared by red mud for phosphate removal. *Desalination, 273*(2–3), 414–420.

Zinatizadeh, A. A. L., Mohamed, A. R., Abdullah, A. Z., Mashitah, M. D., Isa, H. M., & Najafpour, G. D. (2006). Process modeling and analysis of palm oil mill effluent treatment in an up-flow anaerobic sludge fixed film bioreactor using response surface methodology (RSM). *Water Research, 40*(17), 3193–3208.